ISSUE: June 2022

A Guide To Power Electronics Design For Off-Battery Automotive (Part 2): DC-DC Conversion From 12 V

by Timothy Hegarty, Texas Instruments, Phoenix, Ariz.

As mentioned in part 1 of this article series,[1] reliable automotive-grade dc-dc regulator solutions are crucial to the development of automotive ecosystems, powering vehicle loads such as infotainment and cluster, body electronics and lighting, and innovative safety technologies. In that first article I discussed the requirements for immunity against conducted and radiated emissions, ESD and supply-line transients in 12-V and 24-V vehicle electrical systems.

In this second installment, I'll present a voltage regulator design that demonstrates how the immunity requirements can be met in practice and verified. I'll walk through several steps within the context of a power circuit development flow for an automotive application. The steps include creating a list of circuit specifications to meet the application requirements; compiling a schematic and bill of materials; using a calculation or simulation tool to optimize and fine-tune the design; selecting components to achieve low power loss; optimizing board layout to meet electromagnetic interference (EMI) and thermal management constraints; and finally, conducting functional validation and performance testing of the final design.

By way of example, I will delve into an implementation that powers an electronic control module (ECU) with a maximum load current requirement of 15 A. Operating from a 12-V battery supply and based on the LM25141-Q1 synchronous buck controller, the regulator design uses conventional silicon 40-V MOSFETs at a switching frequency of 2.1 MHz to reduce passive component size and avoid operating in the AM radio band. A front-end circuit that includes a reverse-battery protection (RBP) controller (based on the LM74722-Q1 ideal diode controller) enables the system to meet the transient immunity requirements described in detail in part 1, including compliance tests specified in ISO 16750-2, ISO 7637-2 and LV 124.[2]

Circuit Specifications

Table 1 outlines a typical set of system-level specifications for an automotive buck regulator and its front-end protection circuit. Thermal design current (TDC) and electrical design current (EDC) specifications of 10 A and 15 A, respectively, describe the ECU's steady-state and transient load current requirements. Conducted and radiated EMI must meet limits set according to CISPR 25 Class 5.

Table 1. Design specifications for an automotive buck regulator circuit with reverse-battery protection.

Design parameter	**Application specification**
Input voltage range	12-V lead-acid battery (nominal 13.5 V), steady-state range of 8 V to 16 V, cold-crank profile down to 3.8 V and load dump clamped at 35 V
Output voltage setpoint	5 V
Output current	TDC = 10 A, EDC = 15 A and overcurrent protection = 20 A
Quiescent input current	<60 µA at no load and <10 µA when disabled
Buck regulator switching frequency	2.1 MHz (above the AM radio band), allowing a loop bandwidth of 100 kHz
Ambient temperature range	–40°C to 85°C
Bulk storage capacitance	Optional 220 µF for LV 124 E-10 functional Class A performance

Overvoltage cutoff	>35 V
Conducted and radiated EMI	CISPR 25 Class 5 (conducted 150 kHz to 108 MHz and radiated 150 kHz to 5.925 GHz)
Transient immunity compliance	ISO 7637-2, ISO 16750-2 and LV 124
AC voltage superimposed test	6 V peak to peak up to 25 kHz and 2 V peak to peak up to 200 kHz
Battery voltage monitor ratio	8-to-1 attenuation factor

Fig. 1 presents a schematic of a proposed solution to meet the design specifications. The buck power stage includes 40-V power MOSFETs (designated as Q_3 and Q_4) and a 42-V synchronous buck controller (the LM25141-Q1, U_2). The controller has integrated MOSFET gate drivers, ultra-low quiescent operating current and a peak current-mode control architecture. Inductor dc resistance (DCR) current sensing eliminates a 3-mΩ series shunt and its associated power losses, increasing efficiency by 0.8% at 15 A and enabling the inductor to connect directly to the V_{OUT} copper planes on the board for improved thermal performance.

In preparation for board layout,[3] the schematic also identifies high-current connections, high slew-rate voltage nodes, power and analog grounds, and noise-sensitive traces such as those used for current sensing and loop compensation.

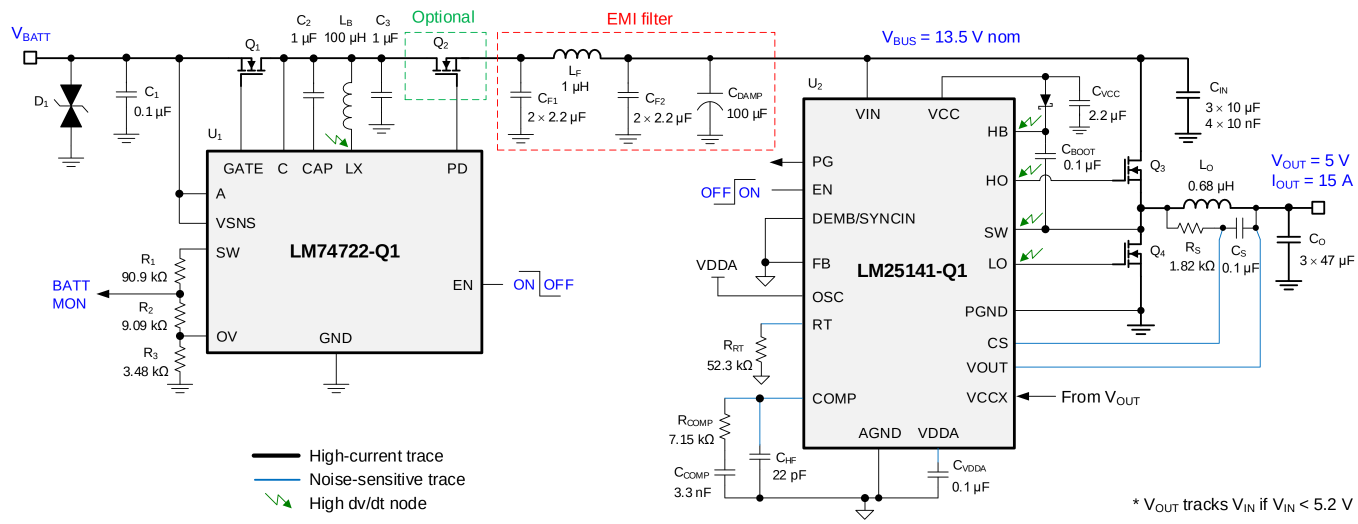

Fig. 1. Schematic of a synchronous buck power stage based on the LM25141-Q1 controller (U_2) and front-end protection circuit based on the LM74722-Q1 ideal diode controller (U_1).

The RBP controller, which uses the Texas Instruments (TI) LM74722-Q1 ideal diode controller, designated as U_1 in Fig. 1, can withstand and protect downstream-connected loads from negative supply voltages, essentially replacing a series Schottky diode. The RBP controller uses two series back-to-back 60-V power MOSFETs connected in a common-drain configuration with independent gate drives, designated as GATE and PD in Fig. 1.

Connected first, an ideal diode MOSFET (Q_1) provides reverse input protection and voltage holdup, followed by an optional second hot-swap MOSFET (Q_2) for power path on-off control, overvoltage clamping protection, inrush current control and load disconnection. With a quiescent current consumption of 27 µA, this circuit can remain always on, obviating the need for a T15 signal from the ignition or a communication (Controller Area Network) bus wakeup signal.[4]

The RBP controller includes an integrated hysteretic-mode boost regulator circuit to provide adequate gate-drive current capability for Q_1 and Q_2, and achieve fast turn-on and turn-off transitions. This circuit ensures reliable performance during automotive testing to meet ISO 16750-2, ISO 7637-2 and LV 124 specifications when an ECU encounters reverse-voltage conditions, micro-short input interruptions, superimposed ac input voltages or other immunity-type events.[1, 2 and 4-6]

Buck Regulator Power-Stage Components

Table 2 details the main bill-of-materials' components for the synchronous buck power stage based on the reference designators (ref des) in Fig. 1. The selected power MOSFETs, buck controller and passive components include qualification to AEC-Q101, AEC-Q100 and AEC-Q200, respectively.

Table 2. Automotive-grade components for the synchronous buck power stage and input EMI filter.

Ref des	**Component**	**Vendor**	**Part number**	**Description**	**Size (mm)**
Q_3	High-side MOSFET	Infineon	IAUC60N04S6L039	40 V, 3.9 mΩ, 7 nC, SON-8	5.1 × 6.1 × 1.0
Q_4	Low-side MOSFET		IAUC80N04S6L032	40 V, 3.2 mΩ, 9 nC, SON-8	
U_2	Buck controller	TI	LM25141-Q1	42-V controller, WQFN-24	4.0 × 4.0 × 0.8
L_O	Buck inductor	Coilcraft	XGL6030-681	0.68 µH, 2.9 mΩ, 22 A	6.7 × 6.5 × 3.1
C_{O1-3}	Output capacitors	Murata	GCM32EC71A476	47 µF, 10 V, X7S, 1210	3.2 × 2.5 × 2.7
		TDK	CGA6P1X7S1A476		
C_{IN1-3}	Input capacitors	AVX	12105C106K4T2A	10 µF, 50 V, X7R, 1210	3.2 × 2.5 × 2.7
		TDK	CNA6P1X7R1H106		
L_F	EMI filter inductor	Coilcraft	XGL4030-102	1 µH, 6.5 mΩ, 10.3 A	4.0 × 4.0 × 3.1
C_{DAMP}	Input damping capacitor	Panasonic	EEEFTH101XAP	100 µF, 50 V, 0.34 Ω	6.3 ϕ × 7.7
C_{F1-4}	EMI filter capacitors	Murata	GCM21BD71H225	2.2 µF, 50 V, X7R, 0805	2.0 × 1.2 × 1.4

Design Tools

There are various easy-to-use tools that simplify and streamline buck regulator design. As an example, Fig. 2 shows a quick-start calculation tool with schematic, Bode plot, efficiency plot and component power-loss estimates.[7] To corroborate the theoretical calculations, Fig. 3 provides a SIMPLIS schematic to facilitate a review of circuit behavior, including but not limited to MOSFET switching, output voltage startup, line and load transient response, Bode plot characteristics, and EMI input filtering.

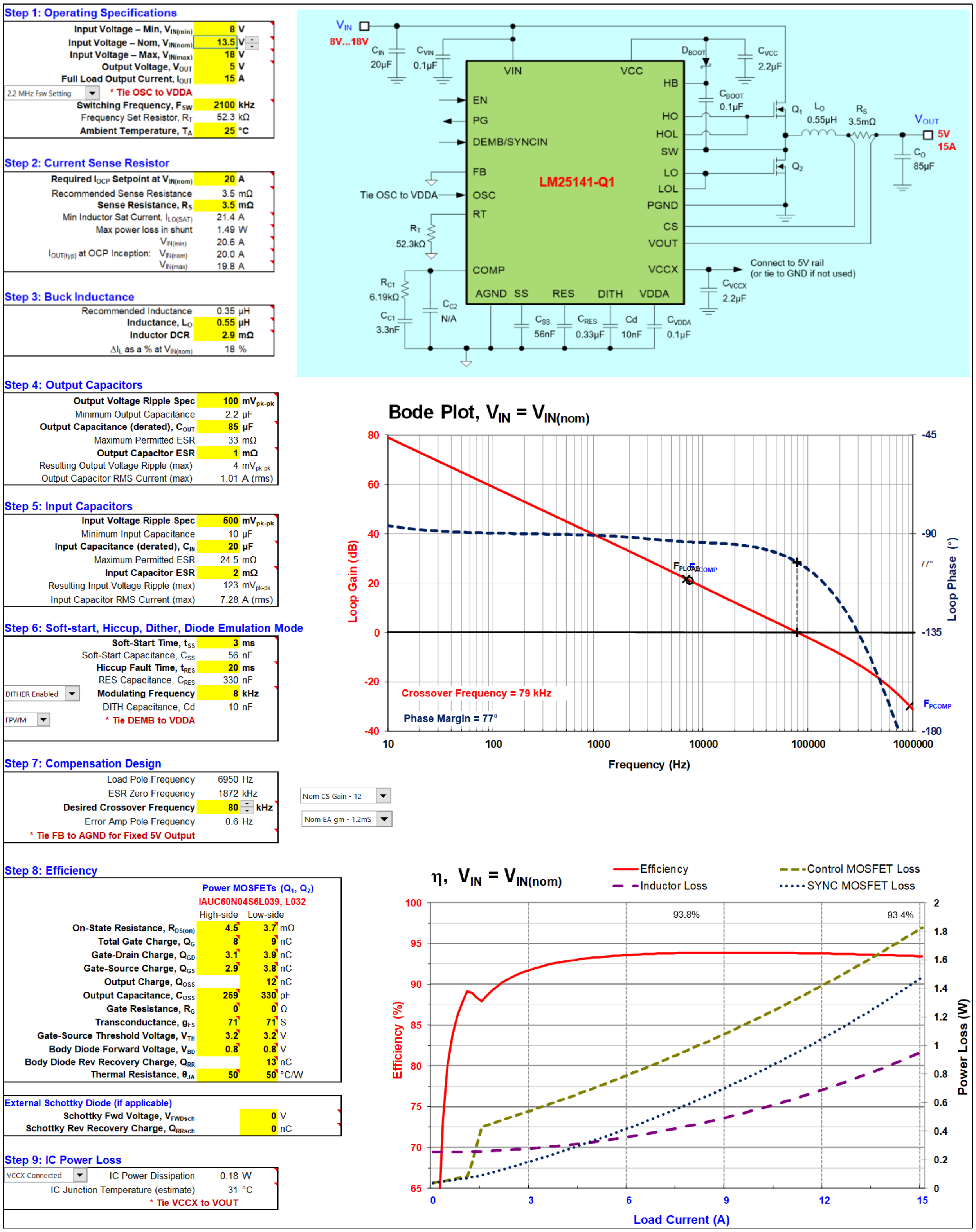

Fig. 2. Controller design tool to assist with component selection, Bode plot analysis and power-loss review.

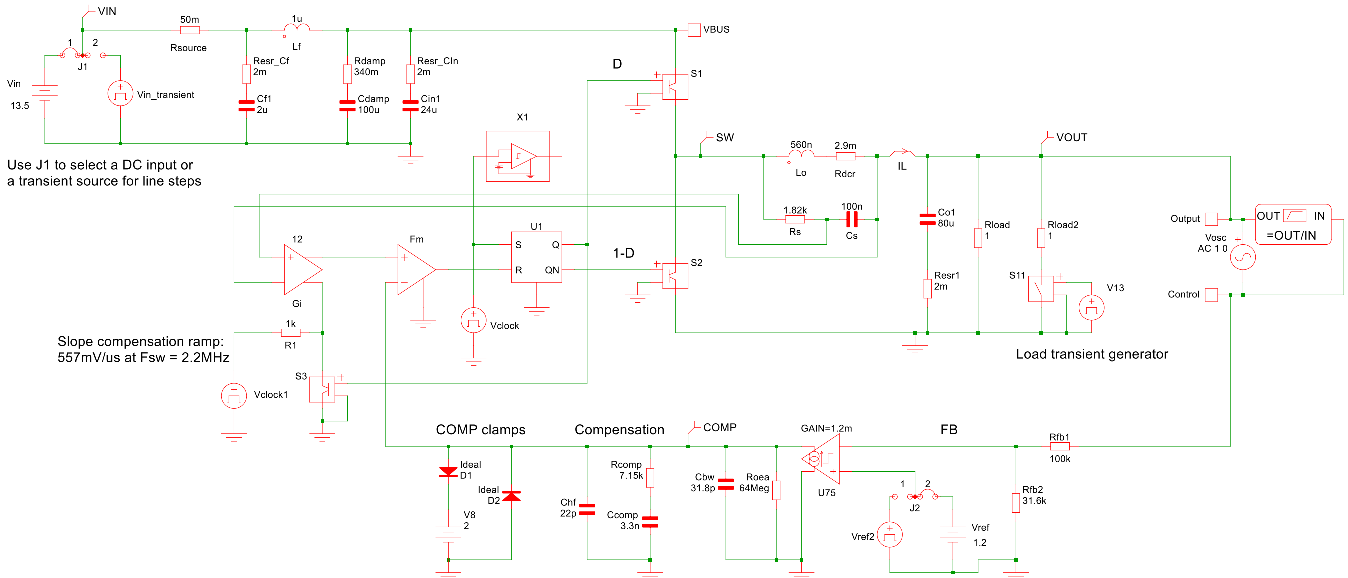

Fig. 3. SIMPLIS simulation schematic to check buck regulator circuit performance.

Buck Regulator Performance

Moving on to the practical implementation, Fig. 4 shows the measured efficiency versus load and line at a switching frequency of 2.1 MHz. The efficiency at a 13.5-V input with load currents of 10 A and 15 A is 94% and 93.2%, respectively. Fig. 5 shows the conducted EMI results that meet CISPR 25 Class 5 specified limits.

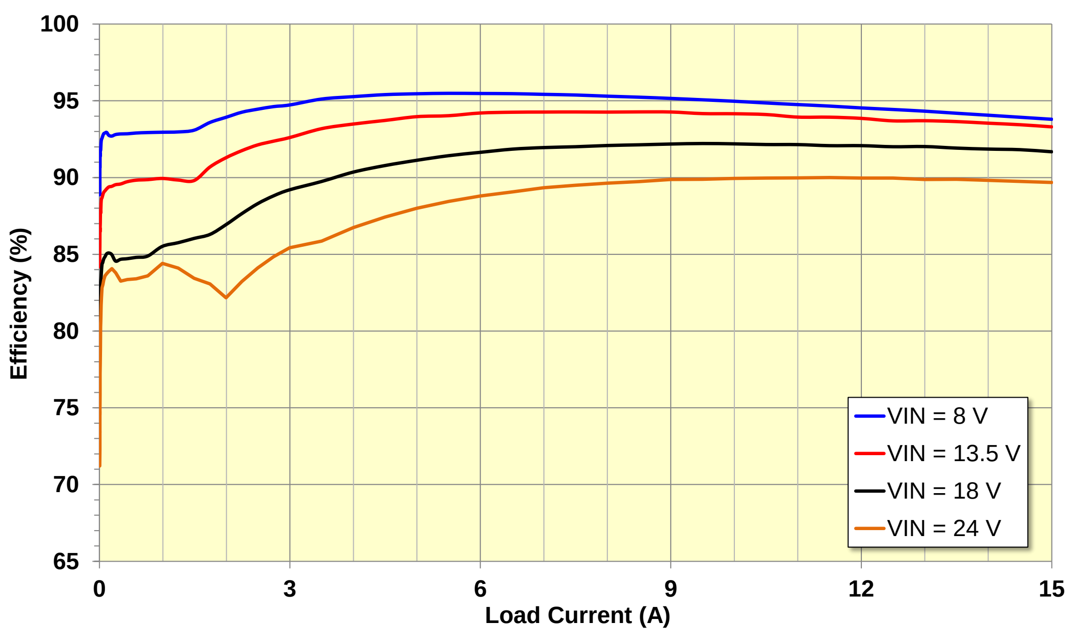

Fig. 4. Efficiency vs. load current at several input voltages with $T_{AMBIENT}$ = 25°C.

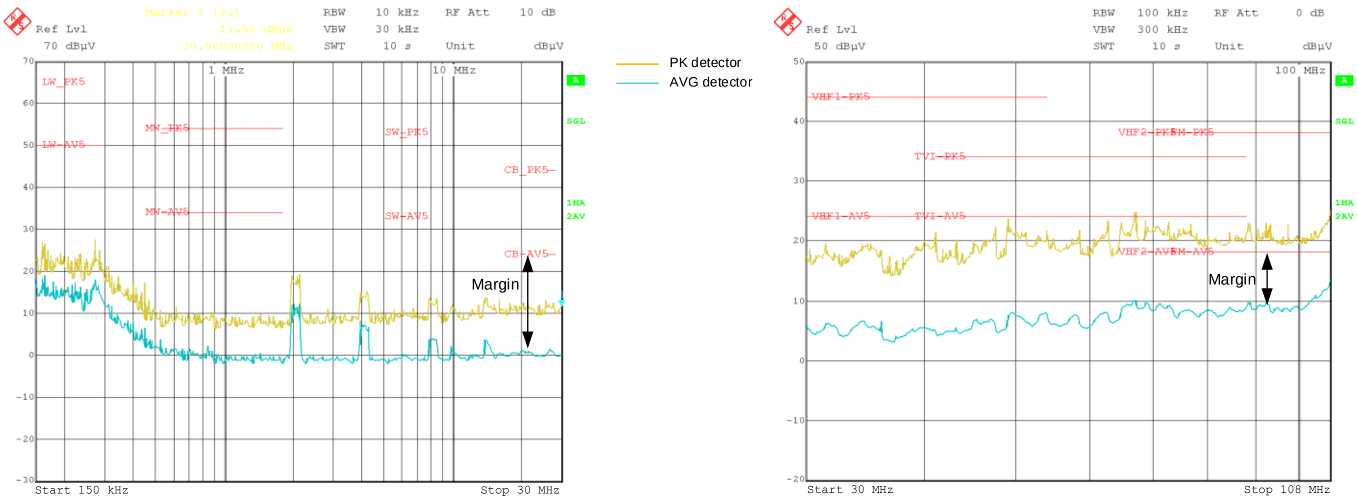

(a) (b)

Fig. 5. CISPR 25 Class 5 conducted EMI results: 150 kHz to 30 MHz (a) and 30 MHz to 108 MHz (b).

Fig. 6 shows a cold-crank starting profile, similar to that described in ISO 16750-2 section 4.6.3 or LV 124 E-11, with the input voltage decreasing to a plateau of 3.8 V for 19 ms. The output voltage continues in dropout approximately 200 mV below the input and subsequently recovers to its 5-V setpoint when the input voltage increases.

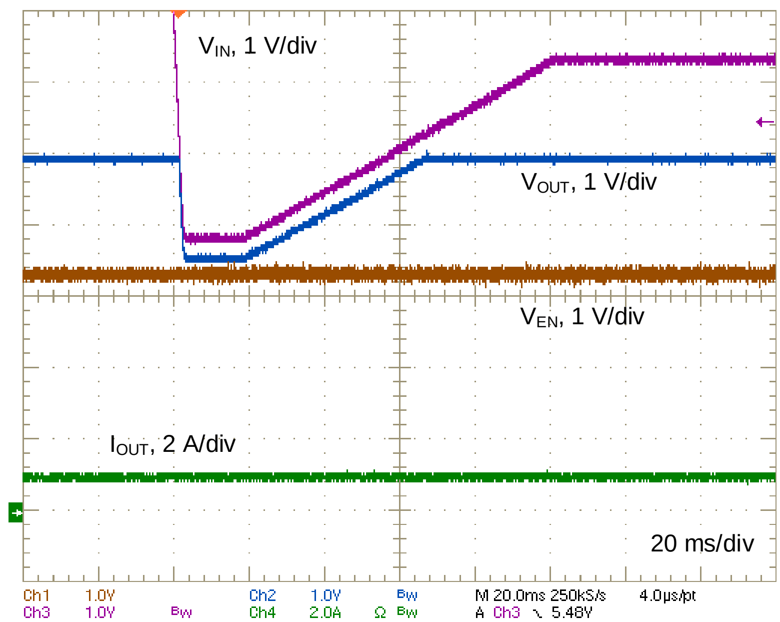

Fig. 6. Cold-crank starting profile with input voltage falling to 3.8 V.

Front-End Protection Circuit

Table 3 itemizes the main bill-of-materials' components for the front-end protection circuit shown in Fig. 1. A transient voltage suppressor (TVS) diode connected across the battery lines provides positive and negative voltage clamping.

Table 3. Automotive-grade components for the reverse-battery protection circuit.

Ref. des.	Component	Vendor	Part number	Description	Size (mm)
Q_1, Q_2	Series MOSFETs	Onsemi	NVMFS5C638NL	60 V, 2.6 mΩ, 7 nC, SO-8	5.1 × 6.1 × 1.0
U_1	RBP controller	TI	LM74722-Q1	RBP controller, WSON-12	3.0 × 3.0 × 0.8
L_B	Boost inductor	Coilcraft	XFL2010-104	100 µH, 6.07 Ω, 172 mA	2.0 × 1.9 × 1.0
D_1	TVS diode clamp	Littelfuse	TPSMB36CA-VR	36 V, 600 W, SMB	5.5 × 3.9 × 2.6
C_2, C_3	Boost circuit input and output capacitors	Murata	GCM21BD71H105	1 µF, 50 V, X7R, 0805	2.0 × 1.2 × 1.5

Reverse Battery And Negative Inductive Voltage Transient Tests

As described in part 1 of this article series, the system must protect against both short- and long-term negative voltage events. More specifically, ISO 16750-2 section 4.7.2.3 includes a description of a negative voltage of −14 V (−28 V for a 24-V system) applied for 1 minute.

Meanwhile, ISO 7637-2 pulse 1 specifies the negative transient immunity of ECUs connected in parallel with a high-current inductive load. Pulse 1 starts when the battery is disconnected where the supply voltage collapses to 0 V, followed by a spike to −150 V with rise and decay times of 1 µs and 2 ms, respectively, which are applied with a source impedance of 10 Ω.

Fig. 7a shows the waveforms with an applied reverse battery voltage of −14 V. Fig. 7b shows the ISO 7637-2 pulse 1 waveform, where a bidirectional TVS diode connected across the input lines clamps the negative transient pulse to −42 V. This is within the maximum operating voltage of U_1 and does not violate the 60-V drain-to-source voltage rating of Q_1.

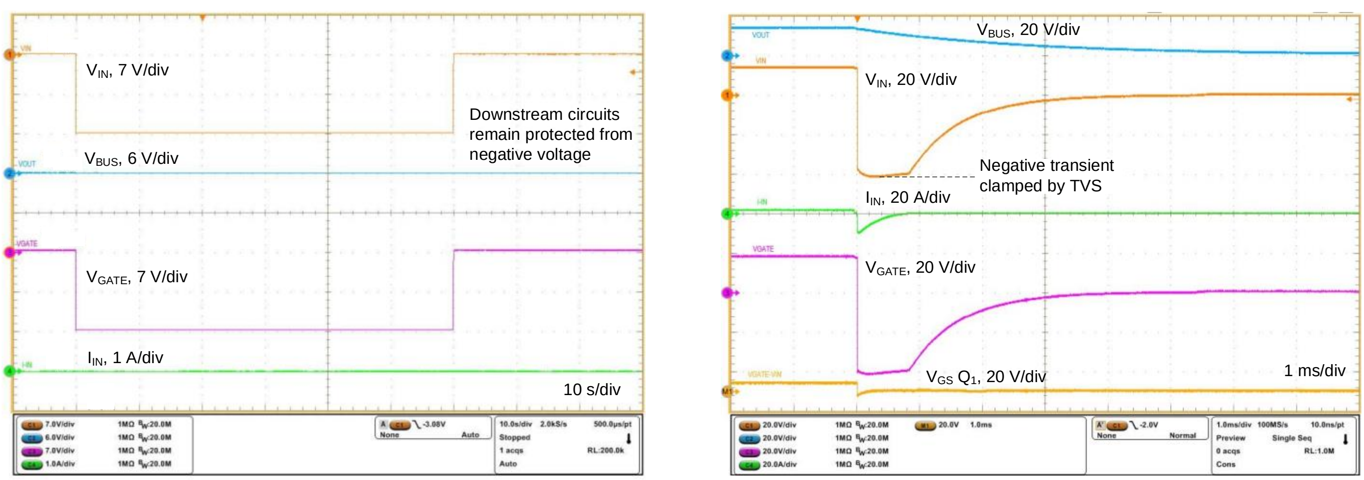

(a) (b)

Fig. 7. MOSFET Q_1 blocks during the reverse-battery voltage test (a) and ISO 7637-2 pulse 1 test (b).

In both cases, the RBP controller blocks reverse current and prevents the bus voltage from swinging negative, protecting the downstream circuits from damage caused by the negative voltage. Q_1 turns off within 0.5 µs when its drain-to-source voltage exceeds a 6.5-mV reverse detection threshold.

Input Micro-Short Interruption Test

Fig. 8 shows the response to an input micro-short transient as specified in LV 124 E-10. Such interruptions can occur during events such as contact and line errors or bouncing. Appropriate sizing of the bulk capacitor provides holdup to achieve functional status Class A performance with no reverse current flow.

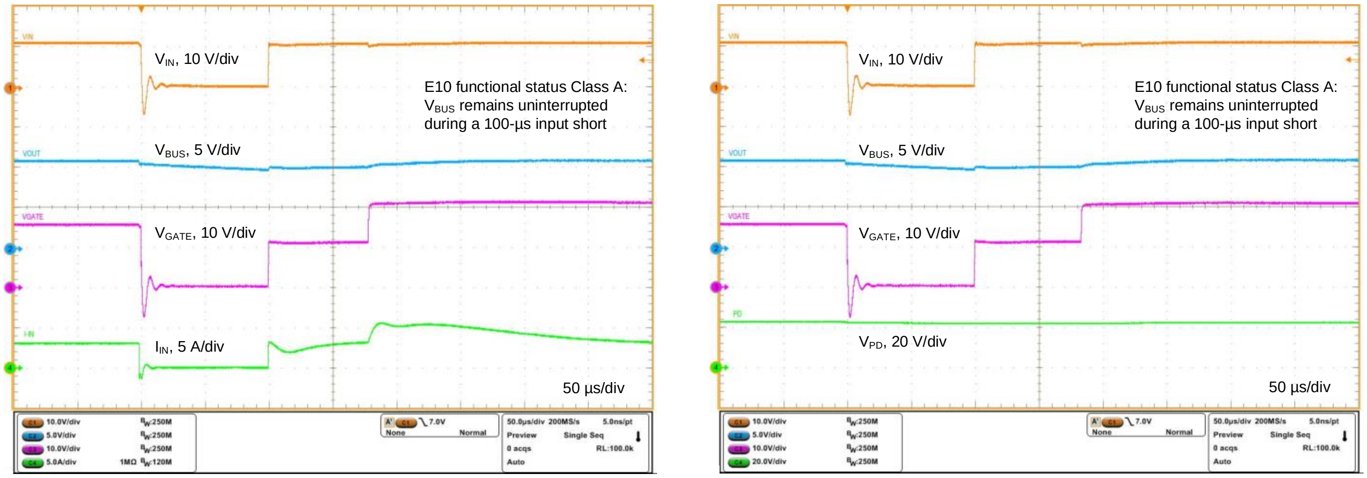

(a) (b)

Fig. 8. LV 124 E-10 input micro-short test waveforms: test case 2 with a 100-µs zero-voltage duration (a) showing the MOSFET Q_2 gate voltage (PD) remaining high in order to facilitate rapid recovery upon removal of the short (b).

AC Superimposed Input Active Rectification Test

ISO 16750-2 section 4.4 and LV 124 E-06 specify ac superimposed tests to verify stable operation of various ECUs with a sinusoidal ripple of 2 V peak to peak on a 13.5-V nominal dc battery voltage, with frequency swept from 50 Hz to 25 kHz. Moreover, original equipment manufacturer-specific requirements such as Volkswagen VW 80000 and Tesla TS-0000425-05 specify a larger amplitude and ripple frequency as high as 200 kHz caused by the upstream dc-dc regulator. Fig. 9 shows two examples of active rectification.

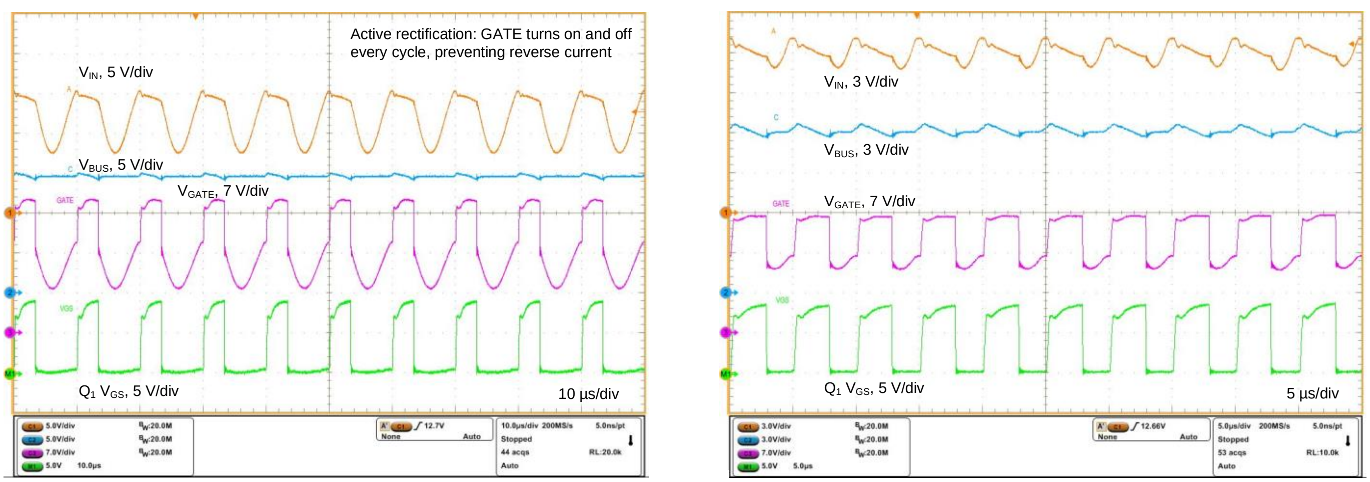

(a) (b)

Fig. 9. Ideal diode MOSFET switching during active rectification of ac superimposed ripple: 6 V peak to peak at 100 kHz (a) and 2 V peak to peak at 200 kHz (b).

The ideal diode MOSFET Q_1 switches off upon the detection of reverse current and switches on when the body diode begins conducting in the forward direction as the current swings positive. The reduced ripple voltage helps automotive audio amplifier and sensor fusion systems in particular, and the lower ripple current amplitude reduces resistive losses in the series MOSFETs and electrolytic bulk capacitor.

Buck Stage And EMI Filter Layout For Minimizing Emissions

The critical aspects of the printed circuit board (PCB) layout relate to the power stage, and Fig. 10a shows the top-side layout of the design. Most automotive designs are multilayer system boards with several ground plane layers for spreading heat. Placing the power-stage components on one side results in lower EMI and simplifies attachment to a heat sink if needed.

Tight layout of the switching loop comprising the input capacitors and power MOSFETs reduces the power-loop parasitic inductance, mitigating switch-voltage overshoot and ringing during MOSFET switching. The MOSFETs' gate drive and gate return traces (HO and SW for Q_3, LO and GND for Q_4) route as differential pairs with minimal loop area. These gate traces are very short, as the controller is close to the MOSFETs. The MOSFETs' switch connection connects immediately to the inductor terminal, and the resulting small switch-node polygon area reduces radiated EMI. The inductor dot signifies the start of the inductor winding and normally connects to the switch node to mitigate radiated fields.

The internal board layers mainly constitute paralleled ground planes for heat sinking and conduction drop reduction. To conveniently connect to the internal ground planes and move heat away from the MOSFETs, multiple thermal vias with a 12-mil diameter hole size connect the high-side MOSFET drain to V_{IN} copper pours that then connect to the EMI filter. Fig. 10b shows a simple EMI filter layout on the bottom side of the PCB, away from the switching components. Filter capacitors (0805 size) in a butterfly arrangement at each corner of the filter inductor tie to the quiet ground plane on the bottom layer.

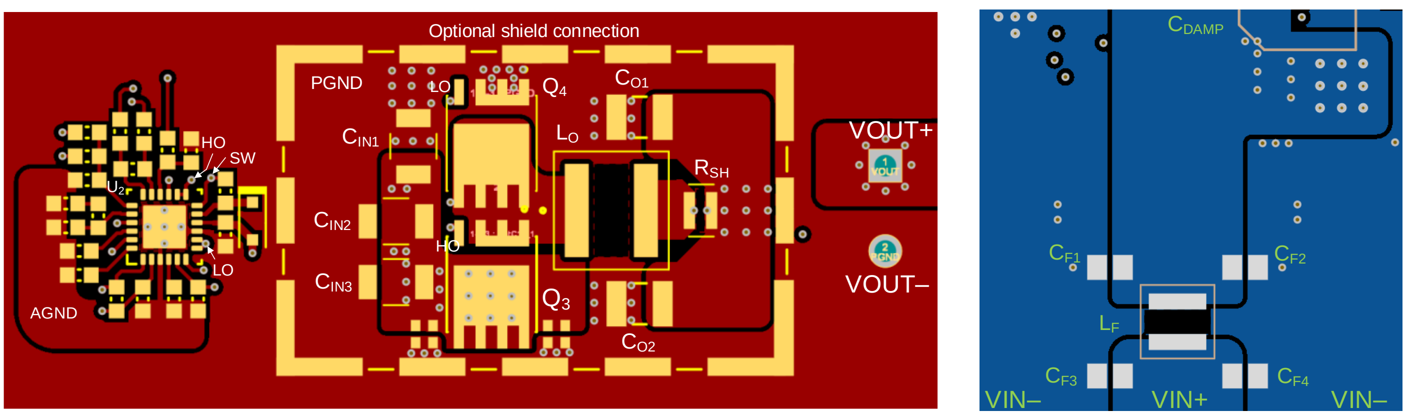

(a) (b)

Fig. 10. Buck power-stage PCB layout (top-down view): top layer (a) and EMI filter on the bottom layer (b).

Summary

A primary objective of this article was to describe the development flow from a designer's perspective of an automotive off-battery power system, with a particular focus on high efficiency, low EMI and reliable transient immunity performance. The article detailed a synchronous buck regulator and front-end protection circuit, providing experimental results and board layout details. The design offers a compact, cost-effective solution based on requirements derived from ISO 16750-2, ISO-7637-2 and LV 124.

In part 3 of this article series, I will describe the applicable electromagnetic compatibility specifications and design of a dc-dc solution for operation from a 48-V battery in a mild hybrid electric vehicle.

References

1. "A Guide To Power Electronics Design For Off-Battery Automotive (Part 1): EMC And Line Transient Requirements" by Timothy Hegarty, How2Power Today, May 2022.
2. "Electric and Electronic Components in Motor Vehicles Up to 3.5 t – General Component Requirements, Test Conditions and Tests." LV 124, Part 1: Electric Requirements and Tests of the 12 V Electric System. 2013.
3. "Improve High-Current DC/DC Regulator EMI Performance for Free with Optimized Power Stage Layout" by Hegarty, Timothy, Texas Instruments application note, literature No. SNVA803, September 2019.
4. "3 Ways to Design a Low Quiescent-Current (I_Q) Automotive Reverse Battery Protection System" by Dilip Jain, TI E2E design support forums technical article, Nov. 18, 2021.
5. "Automotive EMC-Compliant Reverse-Battery Protection with Ideal-Diode Controllers" by Dilip Jain and Abhijeet Godbole, Texas Instruments Analog Design Journal article, literature No. SLYT802, 4Q 2020.
6. "Active Rectification and Its Advantages in Automotive ECU Designs" by Praveen GD, Texas Instruments application brief, literature No. SLVAF88, September 2021.
7. LM25141-Q1 controller quickstart design tool, Texas Instruments, accessed May 24, 2022.

About The Author

Timothy Hegarty is a senior member of technical staff (SMTS) in the Buck Switching Regulators business unit at Texas Instruments. With over 25 years of power management engineering experience, he has written numerous conference papers, articles, seminars, white papers, application notes and blogs.

Tim's current focus is on enabling technologies for high-frequency, low-EMI, isolated and nonisolated regulators with wide input voltage range, targeting industrial, communications and automotive applications in particular. He is a senior member of the IEEE and a member of the IEEE Power Electronics, Industrial Applications and EMC Societies.

For more information on EMI and EMC issues, see How2Power's Power Supply EMI Anthology. Also see the How2Power Design Guide, locate the Design Area category and select "EMI and EMC". For more on dc-dc converter design, see the How2Power Design Guide, locate the Power Supply Function category and select "DC-DC converters".